Autonomous Underwater Vehicles

Dynamics, Developments and Risk Analysis

Robotics Research and Technology

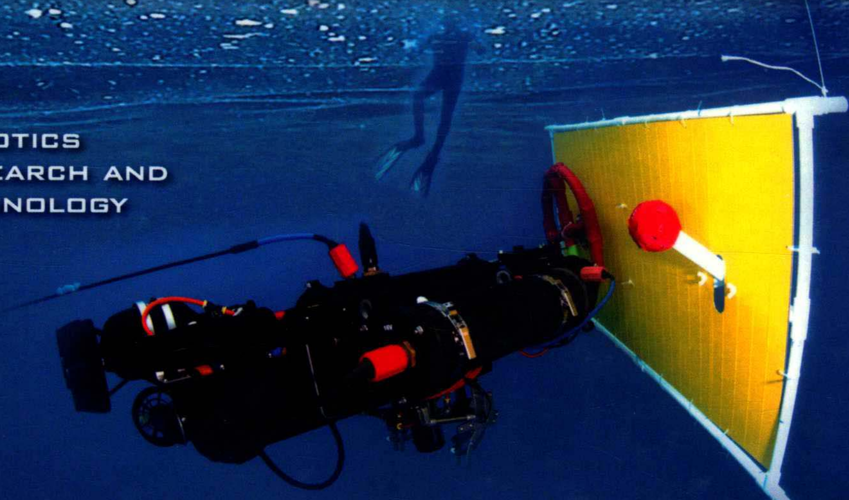

Cynthia Mitchell
Editor

NOVA

ROBOTICS RESEARCH AND TECHNOLOGY

AUTONOMOUS UNDERWATER VEHICLES

DYNAMICS, DEVELOPMENTS AND RISK ANALYSIS

Library of Congress Cataloging-in-Publication Data

ISBN: 978-1-53611-819-3

Published by Nova Science Publishers, Inc. † New York

ROBOTICS RESEARCH AND TECHNOLOGY

Additional books in this series can be found on Nova's website under the Series tab.

Additional e-books in this series can be found on Nova's website under the eBook tab.

ROBOTICS RESEARCH AND TECHNOLOGY

AUTONOMOUS UNDERWATER VEHICLES

DYNAMICS, DEVELOPMENTS AND RISK ANALYSIS

CYNTHIA MITCHELL
EDITOR

nova
science publishers
New York

PREFACE

Gravity-gradient and magnetic-gradient inversion equations are combined to estimate the orientation and distance of an underwater object. The CKF algorithm based on EMMAF algorithm and Spherical-Radial is proposed and is applied to the fault diagnosis of slaver AUV in multi AUV collaborative positioning system. Simulation results are used to analyze the advantages and disadvantages of the three algorithms. This book looks at how a Service-Oriented Agent Architecture (SOAA) for marine robots is endowed with resilient capabilities in order to build a robust (fault-tolerant) vehicle control approach. Particular attention is paid to cognitive RCAs based on agent technologies and any other smart solution already applied or potentially applicable to UMVs. The book also presents current and future trends of RCAs for UMVs.

Chapter 1 - A geophysical inversion information based underwater object detection method is proposed by using the joint Gravity-Gradient and Magnetic-Gradient Inversion algorithms. The gravity-gradient and magnetic-gradient inversion equations are combined to estimate the orientation and distance of the underwater object. After calculating the relative positions of underwater object from the gravity-gradient inversion equations and magnetic-gradient inversion equations, the BP Neural Network is exploited to obtain an optimal geophysical inversion equation applied to underwater object detection. A typical three layered neural network of 6 input and 3 output neurons with a single hidden layer is constructed to realize information fusion. The leading characteristics of such neural network are strong parallel computing, learning and adaptive capabilities, as well as good fault-tolerance. With the proposed method, the trajectories of an underwater object can be detected accurately.

Simulation results show that the authors' method is more efficient than the joint gravity-gradient and magnetic-gradient inversion methods.

Chapter 2 - This chapter introduces the traditional MMAE fault diagnosis algorithm, and illustrates its defects, EMMAEKF can make up its defects, but the EKF algorithm is a sub optimal biased estimate, and for some nonlinear systems, it is difficult to calculate the Jacobian matrix, and in the high dimensional case, the accuracy of UKF is lower. In this chapter, the CKF algorithm based on EMMAF algorithm and Spherical-Radial is proposed and is applied to the fault diagnosis of slaver AUV in multi AUV collaborative positioning system. And simulation results are used to analyze the advantages and disadvantages of the three algorithms.

This chapter introduces the traditional EIMM-CKF fault diagnosis algorithm, and for the system without an accurate model, the filtering accuracy of the system is low and even filter divergence, a EIMM-STCKF algorithm is proposed to diagnose the fault of slaver AUV in multi AUV collaborative positioning system, and the EIMM-MSTCKF algorithm is proposed for the fault diagnosis of slaver AUV in the collaborative positioning of AUV in order to improve the positioning accuracy, the simulation results are used to analyze the advantages and disadvantages of the three algorithms.

Chapter 3 - State-of-the-art technologies for ocean engineering are currently based on autonomous solutions to tackle more complex maritime missions by means of adaptation capabilities. This chapter presents how a Service-Oriented Agent Architecture (SOAA) for marine robots is endowed with resilient capabilities in order to build a robust (fault-tolerant) vehicle control approach. The SOAA is based on two Information Technology (IT) paradigms for modern computing systems: service-oriented architecture and agent technology. The former mainly provides flexibility for dynamic reconfiguration. The latter particularly provides intelligent autonomy based on knowledge representation for situation awareness. This architectural approach moves away from fixed mission plans and very basic diagnostics schemes. It is able to handle unexpected faults at vehicle, sensor and sensor processing levels based on either hardware failure or environmental changes. This chapter provides a description of methods for on-board diagnosis and mitigation of faults. The operation context, and fault cases from different scenarios are presented. Remarking conclusions and future research work are also discussed.

Chapter 4 - The state of the art of Robotic Control Architectures (RCAs) presented in this Chapter not only focuses on ocean engineering but also takes into account other robotics areas that can strongly contribute to RCAs for Unmanned Marine Vehicles (UMVs). Particular attention is paid to cognitive

RCAs based on agent technologies and any other smart solution already applied or potentially applicable to UMVs. The justification of this survey direction is underpinned by the relevance of these architectural approaches in the late years. Addressing the above context, two main classifications for RCAs can be made: (1) situation awareness and autonomy, and (2) number of autonomous computing units. The former is for those approaches that rigorously follow an intelligent autonomy architecture, and in particular those which really propose autonomous RCAs. The latter is according to the amount of agents or self-governed entities implemented per UMV or team of UMVs. The main aspects of interest discussed in this chapter are linked to the support from the RCAs reviewed for: intelligent autonomy, computing paradigm, and technology development. This chapter also presents current and future trends of RCAs for UMVs.

CONTENTS

In: Autonomous Underwater Vehicles ISBN: 978-1-53611-819-3
Editor: Cynthia Mitchell

Chapter 1

UNDERWATER OBJECT DETECTION BASED ON GEOPHYSICAL INVERSION INFORMATION

Ying Weng[1,*], PhD and Meng Wu[2], PhD

[1]School of Computer Science, Bangor University, Bangor, Gwynedd, UK

[2]School of Remote Sensing and Information Engineering, Wuhan University, Wuhan, Hubei, China

ABSTRACT

A geophysical inversion information based underwater object detection method is proposed by using the joint Gravity-Gradient and Magnetic-Gradient Inversion algorithms. The gravity-gradient and magnetic-gradient inversion equations are combined to estimate the orientation and distance of the underwater object. After calculating the relative positions of underwater object from the gravity-gradient inversion equations and magnetic-gradient inversion equations, the BP Neural Network is exploited to obtain an optimal geophysical inversion equation applied to underwater object detection. A typical three layered neural network of 6 input and 3 output neurons with a single hidden layer is constructed to realize information fusion. The leading characteristics of such neural network are strong parallel computing, learning and adaptive capabilities, as well as good fault-tolerance. With the proposed method, the trajectories of an underwater object can be detected accurately.

* Corresponding Author: y.weng@bangor.ac.uk.

Simulation results show that our method is more efficient than the joint gravity-gradient and magnetic-gradient inversion methods.

Keywords: magnetic gradient inversion, gravity gradient inversion, underwater object detection, BP neural network

1. UNDERWATER OBJECT DETECTION BASED ON GRAVITY GRADIENT

This section describes the automated gravity gradient tensor inversion algorithm (AGGTI). The algorithm considers and combines full-tensor gravity gradient components. With this algorithm, the mass and center location of an object with an arbitrary shape and density can be quantified simultaneously using the gravity gradient anomalies induced by the object, which is useful to gain new information about the object. Unlike radar, laser and sonar, the gravity gradiometer cannot be easily detected and interfered with due to the covertness of the submarine. The submarine does not need to float near the surface. AGTI algorithm is applied to a complicated model of an abnormal object with measurement errors and interference from the near smaller illusive object. Experimental results show that the method is convenient for implementation and works well even if the data contain errors and interference.

1.1. Mathematical Foundation

The gravity anomaly at the field point $P(x, y, z)$ caused by an object can be described as:

$$\begin{aligned}\Delta g(x,y) &= G\iiint \frac{\Pi(\xi,\eta,\zeta)\rho(\xi,\eta,\zeta)(\zeta-z)}{[(\xi-x)^2+(\eta-y)^2+(\zeta-z)^2]^{3/2}}d\xi d\eta d\zeta \\ &= G\iiint \Pi(q)\rho(q)K(p,q)d\xi d\eta d\zeta\end{aligned} \tag{1.1}$$

where (ξ,η,ζ) is the positional coordinates of the object. $\Pi(\xi,\eta,\zeta)$ is the geometrical function determined by the object's boundary. The value of the function is 1 if the object is on the boundary; otherwise, the value of the function is 0. $\rho(\xi,\eta,\zeta)$ is the density contrast distribution function. The geometrical and physical parameters of the object can be acquired by $\Pi(\xi,\eta,\zeta)$ and $\rho(\xi,\eta,\zeta)$. G is the universal gravitational constant [4].

The underwater object detection technology based on gravity gradient considers the object as a 3D body with density contrast and the object detection as gravity gradient inversion. Therefore, the problem is converted into the gravity gradient inversion of the object's geometrical and physical parameters. Figure 1.1 shows the Cartesian reference frame used to specify the source and field points [4, 6].

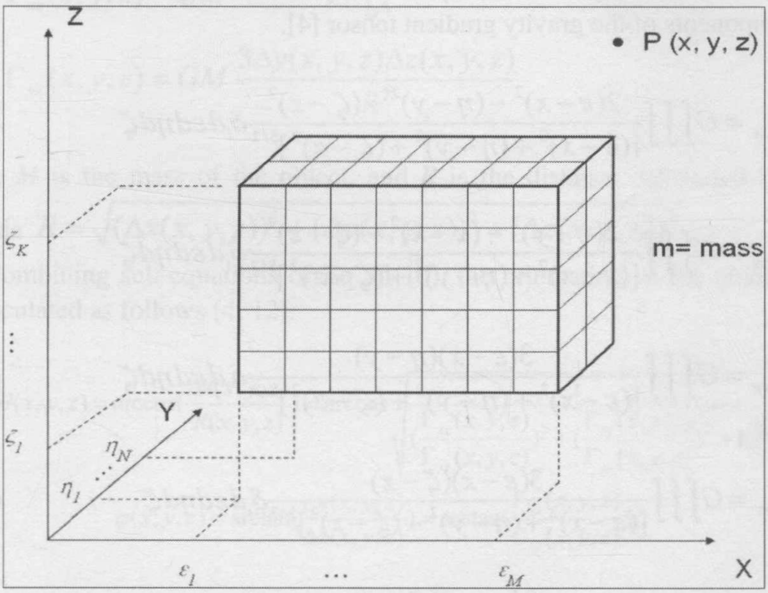

Figure 1.1. Cartesian Reference Frame used to Specify Source and Field Points.

The x - y plane is taken as horizontal axes and the z-axis as vertical. The increasing value of z represents the increasing height. If a particle with its mass m is at the point $o(\xi,\eta,\zeta)$ and δ_i is a assigned value for its density, the gravitational potential Φ at the field point $P(\xi,\eta,\zeta)$ caused by the object (the inertial centrifugal force is negligible here) can be described as the gravity potential Φ at the field point $P(x,y,z)$ (the inertial centrifugal force is negligible here). The operation can be described as following equations [4, 5]:

$$\Phi = \frac{Gm}{r} = \frac{Gm}{\sqrt{(\varepsilon - x)^2 + (\eta - y)^2 + (\varsigma - z)^2}} \tag{1.2}$$

$$\frac{\partial \Phi}{\partial z} = Gm \frac{(\varsigma - z)}{[(\varepsilon - x)^2 + (\eta - y)^2 + (\varsigma - z)^2]^{3/2}} \tag{1.3}$$

$$\frac{\partial^2 \Phi}{\partial z^2} = Gm \frac{2(\varsigma - z)^2 - (\varepsilon - x)^2 - (\eta - y)^2}{[(\varepsilon - x)^2 + (\eta - y)^2 + (\varsigma - z)^2]^{5/2}} \tag{1.4}$$

By differentiating Φ with respect to x, y and z, it is possible to derive the six components of the gravity gradient tensor [4].

$$\Gamma_{xx} = G\iiint \frac{2(\varepsilon - x)^2 - (\eta - y)^2 - (\zeta - z)^2}{[(\varepsilon - x)^2 + (\eta - y)^2 + (\zeta - z)^2]^{5/2}} \delta_i d\varepsilon d\eta d\zeta \tag{1.5}$$

$$\Gamma_{yy} = G\iiint \frac{2(\eta - y)^2 - (\varepsilon - x)^2 - (\zeta - z)^2}{[(\varepsilon - x)^2 + (\eta - y)^2 + (\zeta - z)^2]^{5/2}} \delta_i d\varepsilon d\eta d\zeta \tag{1.6}$$

$$\Gamma_{xy} = G\iiint \frac{3(\varepsilon - x)(\eta - y)}{[(\varepsilon - x)^2 + (\eta - y)^2 + (\zeta - z)^2]^{5/2}} \delta_i d\varepsilon d\eta d\zeta \tag{1.7}$$

$$\Gamma_{xz} = G\iiint \frac{3(\varepsilon - x)(\zeta - z)}{[(\varepsilon - x)^2 + (\eta - y)^2 + (\zeta - z)^2]^{5/2}} \delta_i d\varepsilon d\eta d\zeta \tag{1.8}$$

$$\Gamma_{yz} = G\iiint \frac{3(\eta - y)(\zeta - z)}{[(\varepsilon - x)^2 + (\eta - y)^2 + (\zeta - z)^2]^{5/2}} \delta_i d\varepsilon d\eta d\zeta \tag{1.9}$$

If the distance between the object and the field point is long enough to ignore the size of the object, Eq. (1.5) - Eq. (1.9) can be written as:

$$\begin{cases} \Gamma_{xx}(x,y,z) = GM\dfrac{3(\Delta x(x,y,z))^2 - R^2}{R^5} \\ \Gamma_{yy}(x,y,z) = GM\dfrac{3(\Delta y(x,y,z))^2 - R^2}{R^5} \\ \Gamma_{zz}(x,y,z) = GM\dfrac{3(\Delta z(x,y,z))^2 - R^2}{R^5} \\ \Gamma_{xy}(x,y,z) = GM\dfrac{3\Delta x(x,y,z)\Delta y(x,y,z)}{R^5} \\ \Gamma_{xz}(x,y,z) = GM\dfrac{3\Delta x(x,y,z)\Delta z(x,y,z)}{R^5} \\ \Gamma_{yz}(x,y,z) = GM\dfrac{3\Delta y(x,y,z)\Delta z(x,y,z)}{R^5} \end{cases} \quad (1.10)$$

where M is the mass of the object, and R is the distance calculated by the formula $R = \sqrt{(\Delta x(x,y,z))^2 + (\Delta y(x,y,z))^2 + (\Delta z(x,y,z))^2}$

Combining sub equations of Eq. (1.10), the orientation of the object can be calculated as follows [4, 12]:

$$\begin{cases} \theta(x,y,z) = \arccos(\dfrac{\Delta z(x,y,z)}{R(x,y,z)}) = \arccos\sqrt{\dfrac{1}{(\dfrac{\Gamma_{xy}(x,y,z)}{\Gamma_{yz}(x,y,z)})^2 + (\dfrac{\Gamma_{xy}(x,y,z)}{\Gamma_{xz}(x,y,z)})^2 + 1}} \\ \varphi(x,y,z) = \arctan(\dfrac{\Delta y(x,y,z)}{\Delta z(x,y,z)}) = \arctan(\dfrac{\Gamma_{yz}(x,y,z)}{\Gamma_{xz}(x,y,z)}) \end{cases} \quad (1.11)$$

$$R(x,y,z) = \sqrt[3]{\frac{GM}{\Gamma_{xx}(x,y,z) + \Gamma_{yy}(x,y,z)}(1 - \frac{3}{(\dfrac{\Gamma_{xy}(x,y,z)}{\Gamma_{yz}(x,y,z)})^2 + (\dfrac{\Gamma_{xy}(x,y,z)}{\Gamma_{xz}(x,y,z)})^2 + 1})} \quad (1.12)$$

1.2. Simulation Experiments and Results

In building a simulation model, many cubic blocks are stacked together to create a large 3D object. Each cube is $1m^3$ in size and assigned a value for its density. This creates a 3D model of the object with realistic features [4].

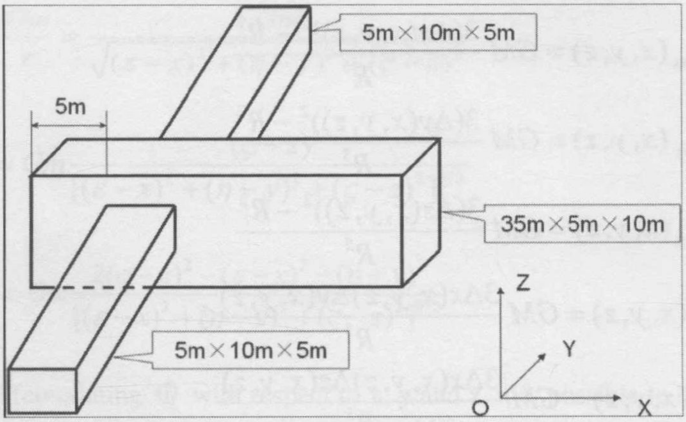

Figure 1.2. Modeling 3D Cube Blocks.

Figure 1.2 shows the 3D cube blocks modeling and Table 1.1 gives the size and density contrast values assigned to the object units. The mass distribution of the object is symmetrically assumed to ensure that the density contrast is constantly distributed, rather than spatially.

Table 1.1. Geometrical and Physical Parameters of the Model

Length (m)	Height (m)	Width (m)	Mass (t)	Density contrast (t/m^3)
35.0	10.0	25.0	70.0	0.0311

If the object is in its resting state, the gravity gradient tensor responses on the measurement plane can be measured by a gravity gradiometer which is carried on an autonomous underwater vehicle (AUV). In the survey area, as the AUV moves, the data are acquired at every survey point which is spaced 1m along both *x* and *y* orientations. As a result, the bigger the survey area is, the more data are acquired. Table 1.2 shows the influence of the survey area on the estimation of the object's mass.

It can be seen that the bigger the survey area is, the more accurate the mass estimation is. We can acquire the mass' magnitude with much smaller survey area. Therefore, the detection may be predigested [4, 6].

The estimated track of the object is described in Figure 1.3 in pentagrams. Statistically, the average distance between the object actual position and gravity gradiometer is 192.17m, with 48.57% estimation error of object mass. The average estimation error of the track in the *x*-direction and *y*-direction is 18.89% and 18.01%, respectively [4].

Table 1.2. Influences of the Survey Area on the Estimation of the Mass of the Object

Survey area (m^2)	Estimation of Mass (t)
64*64	3.694
128*128	16.686
192*192	28.384
256*256	36.622
384*384	46.530
512*512	52.043
768*768	57.849
1024*1024	60.838
1536*1536	63.868
2048*2048	65.394
3072*3072	66.926
4096*4096	67.694

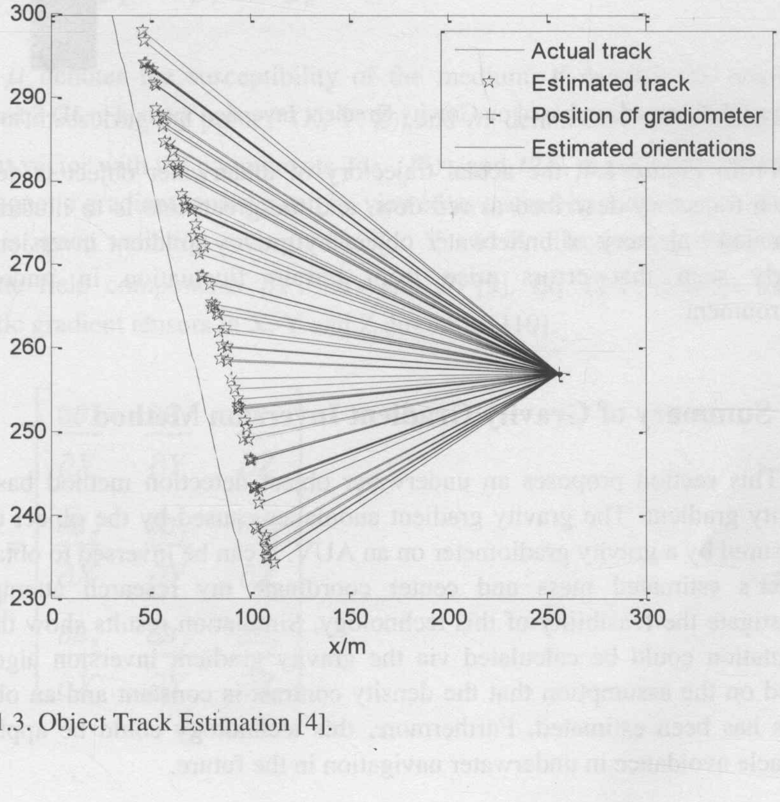

Figure 1.3. Object Track Estimation [4].

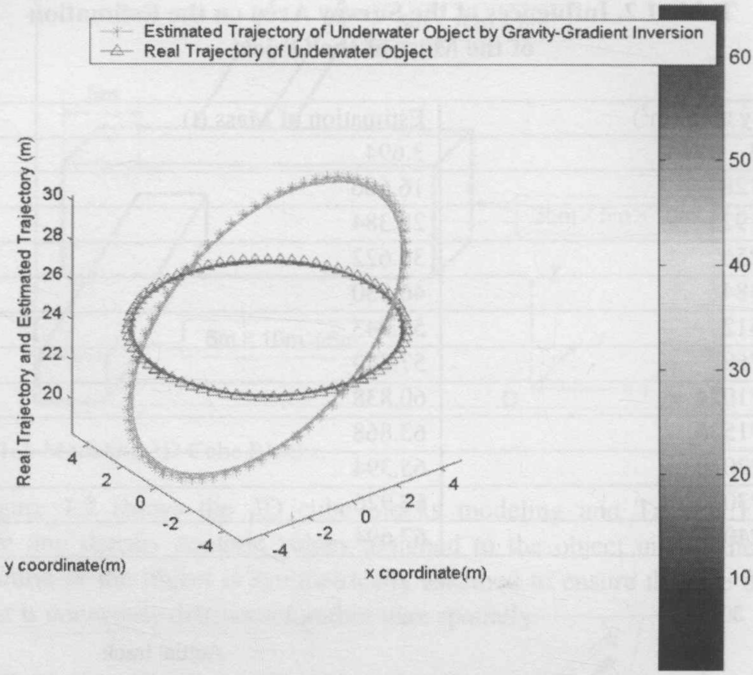

Figure 1.4. Comparison based on Gravity Gradient Inversion method in 3D Space.

From Figure 1.4, the actual trajectory of underwater object is depicted with a trajectory described as red dots, and the green line is to illustrate the estimated trajectory of underwater object by gravity gradient inversion. It is clearly seen that errors arise from terrain fluctuation in underwater environment.

1.3. Summary of Gravity Gradient Inversion Method

This section proposes an underwater object detection method based on gravity gradient. The gravity gradient anomalies caused by the object can be measured by a gravity gradiometer on an AUV. It can be inversed to obtain the object's estimated mass and center coordinate my research attempts to investigate the feasibility of this technology. Simulation results show that the orientation could be calculated via the gravity gradient inversion algorithm based on the assumption that the density contrast is constant and an object's mass has been estimated. Furthermore, this technology could be applied in obstacle avoidance in underwater navigation in the future.